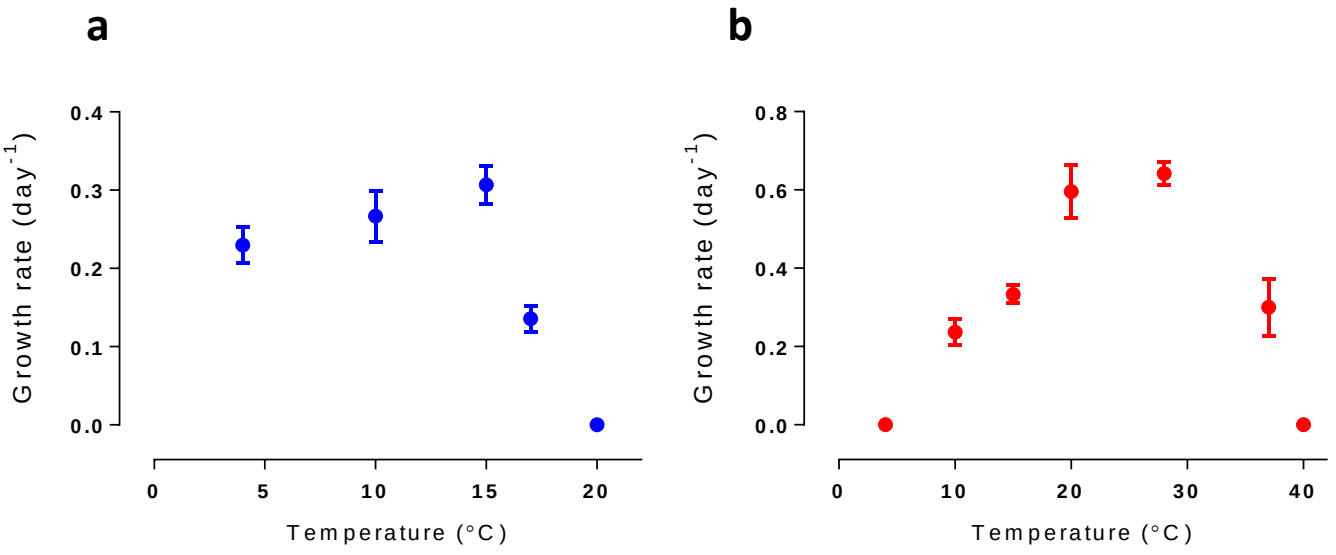


**Figure 1.** The maximal growth rate of exponentially growing algal cultures at various temperatures**. (a)** *Chlamydomonas* sp. UWO241 **(b)** *Chlamydomonas reinhardtii*. Data are the means ± SD of at least six biological replicates

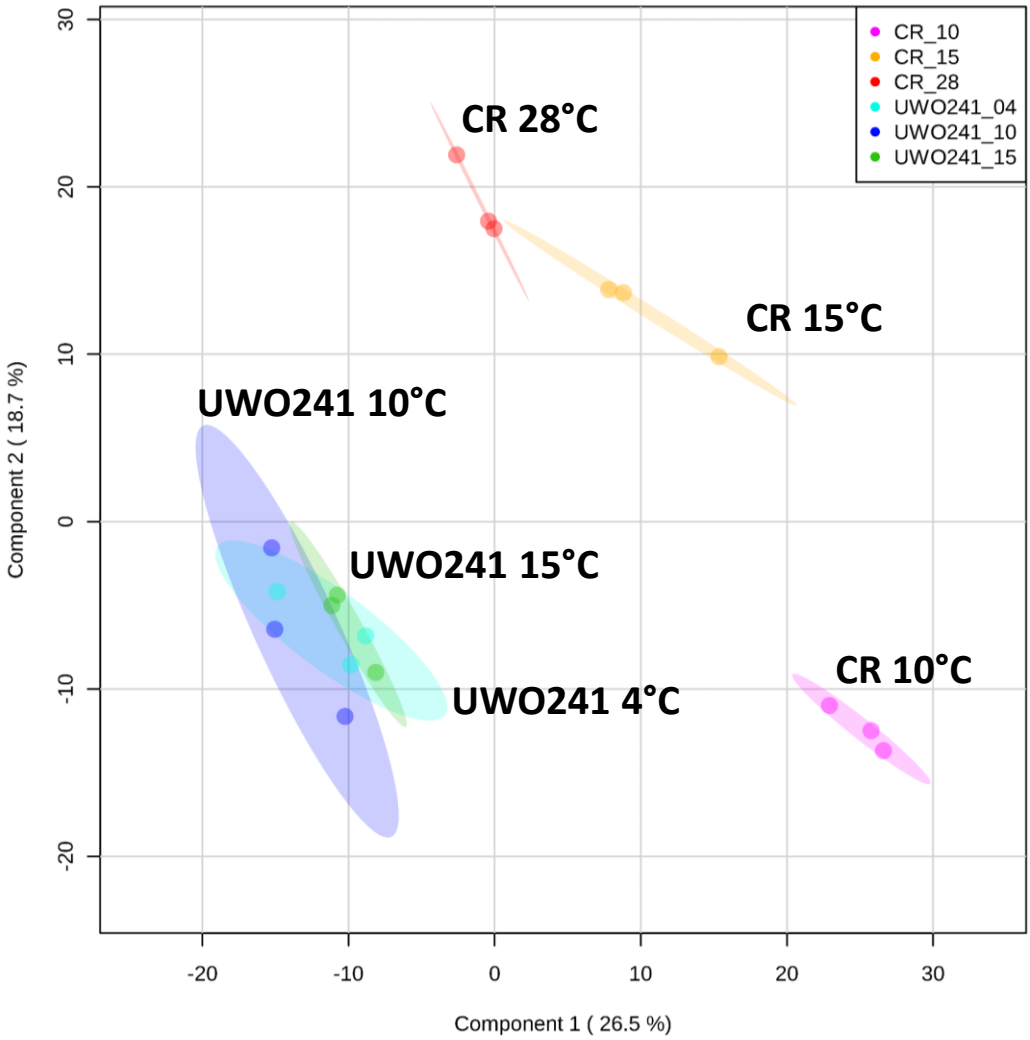


**Figure 2:** Principal component analysis (PCA) of the primary metabolome of the two *Chlamydomonas* species acclimated to different steady-state temperatures. *C. reinhardtii* was grown at 10°C (magenta; CR_10), 15°C (orange; CR_15), and 28°C (red; CR_28). UWO241 was grown at 4°C (cyan; UWO241_04), 10°C (blue; UWO241_10) and 15°C (green; UWO241_15). The analysis includes all 771 quantified metabolites separated along the first two principal components that explained the largest degree of variation in the datasets, and the 95% confidence interval for each treatment.

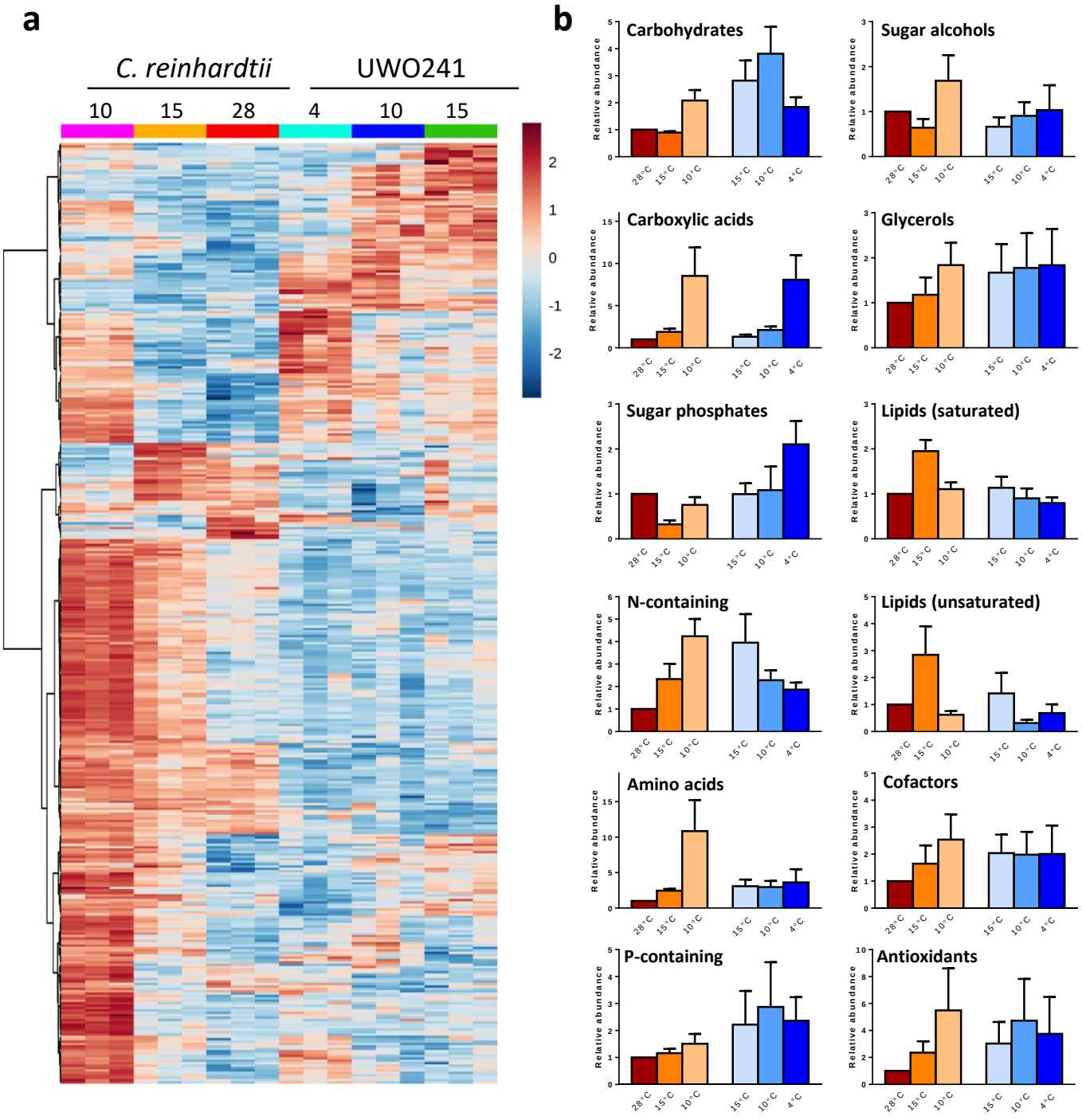


**Figure 3.** Differences in the primary metabolome of *C. reinhardtii* and UWO241, acclimated at different steady-state temperatures. (**a**) Heat map showing the relative changes in metabolite abundances between growth temperatures in the two algal species. Only metabolites which are significantly different are shown (392 metabolites, ANOVA, P<0.01). In each treatment, three biological replicates are represented using a color based metabolite profile as indicated (red – increase in abundance; blue – decrease in abundance). Hierarchical clustering is based on Euclidean distances and Ward's linkage. (**b**) Relative abundance of metabolites classified based on their chemical nature. Only metabolites which were positively identified based on their GC-MS spectra and retention times were taken into consideration. In this analysis, the metabolite abundance corresponding to *C. reinhardtii* grown at 28°C was arbitrarily set to 1 and all other treatments were compared to this sample.

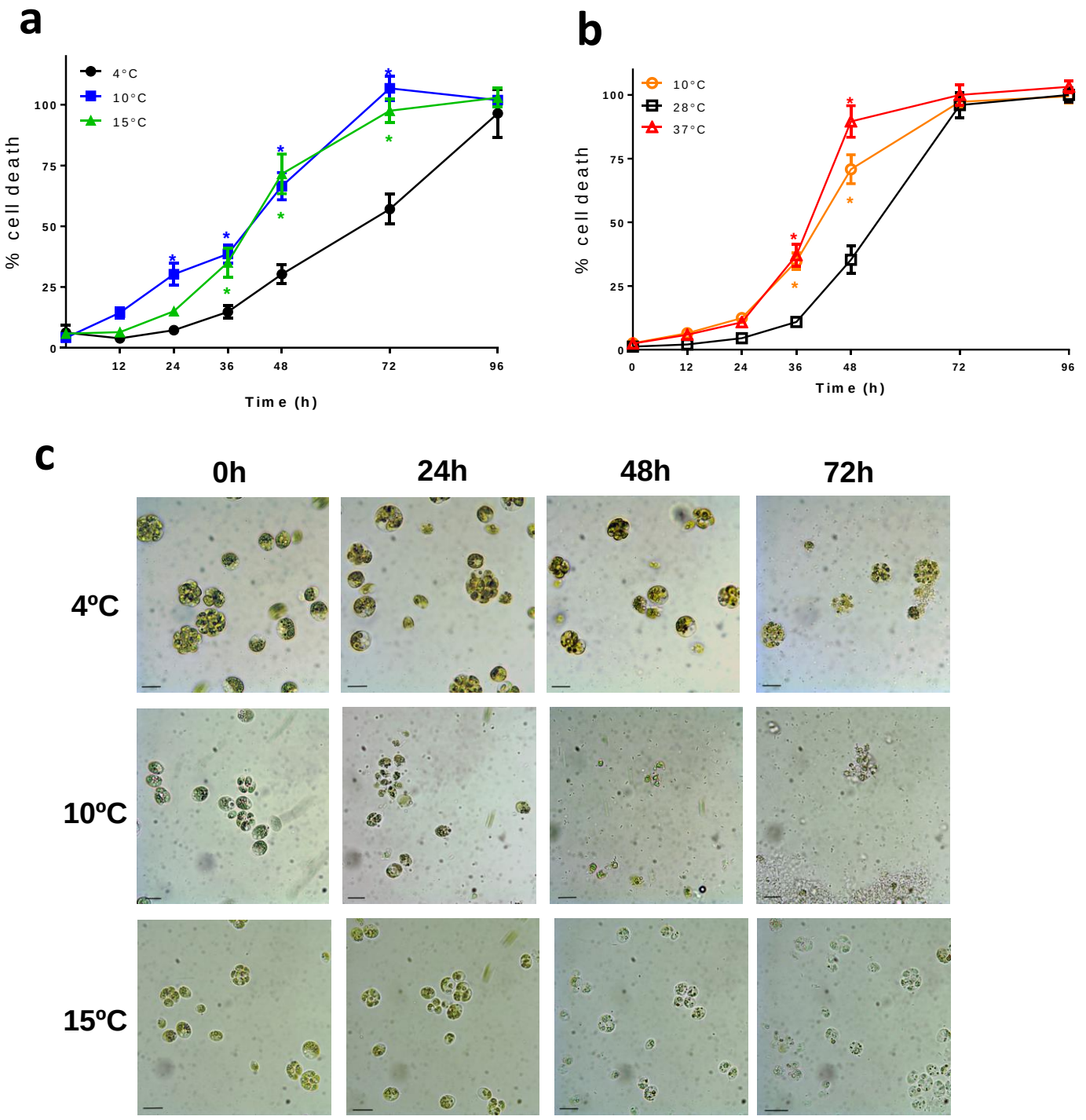


**Figure 4.** Kinetics of cell death in UWO241 **(a)** and *C. reinhardtii* **(b)** acclimated to different growth temperatures and exposed to non-permissive conditions (24°C and 42°C, respectively). Cell death was estimated as a percentage of algal cells stained with 0.5% Evans Blue that accumulates in cells with damaged membranes. Algal cells treated with 1% v/v chloroform were taken as a positive control and used to calculate 100% cell death. Data are means ± SD of at least three independent experiments and analyzed by two-way ANOVA followed by Bonferroni post-test comparing each treatment with 4°C (UWO241) and 28°C (*C. reinhardtii*). Statistical significance ($P<0.01$) is indicated as * **(c)** Light microscope images of UWO241 acclimated to different steady state temperatures (4°C, 10°C, 15°C) and exposed to non-permissive temperature (24°C) for 24h, 48h and 72h. Algae are present as single cells or palmelloid colonies. Scale bar = 15 μm (400x total magnification)

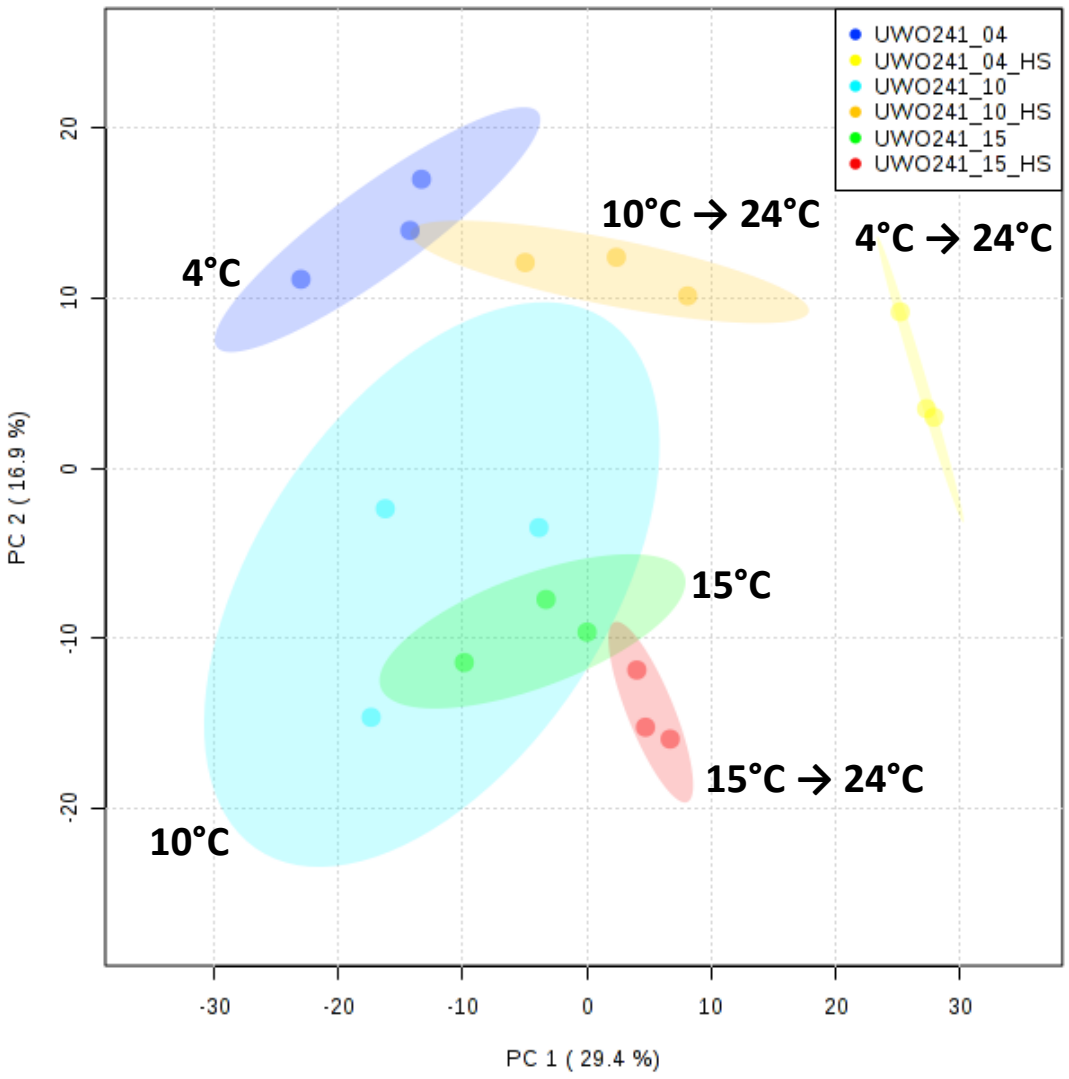


**Figure 5.** Principal component analysis (PCA) of the primary metabolome of UWO241 acclimated to different steady-state temperatures and subsequently exposed to non-permissive temperature for 6 hours. UWO241 was grown at 4°C (blue, UWO241_4) and exposed to 24°C (yellow, UWO241_4_HS); grown at 10°C (cyan; UWO241_10) and exposed to 24°C (orange, UWO241_10_HS); and grown at 15°C (green; UWO241_15) and exposed to 24°C (red, UWO241_15_HS). The analysis includes all quantified metabolites separated along the first two principal components and the 95% confidence interval for each treatment.

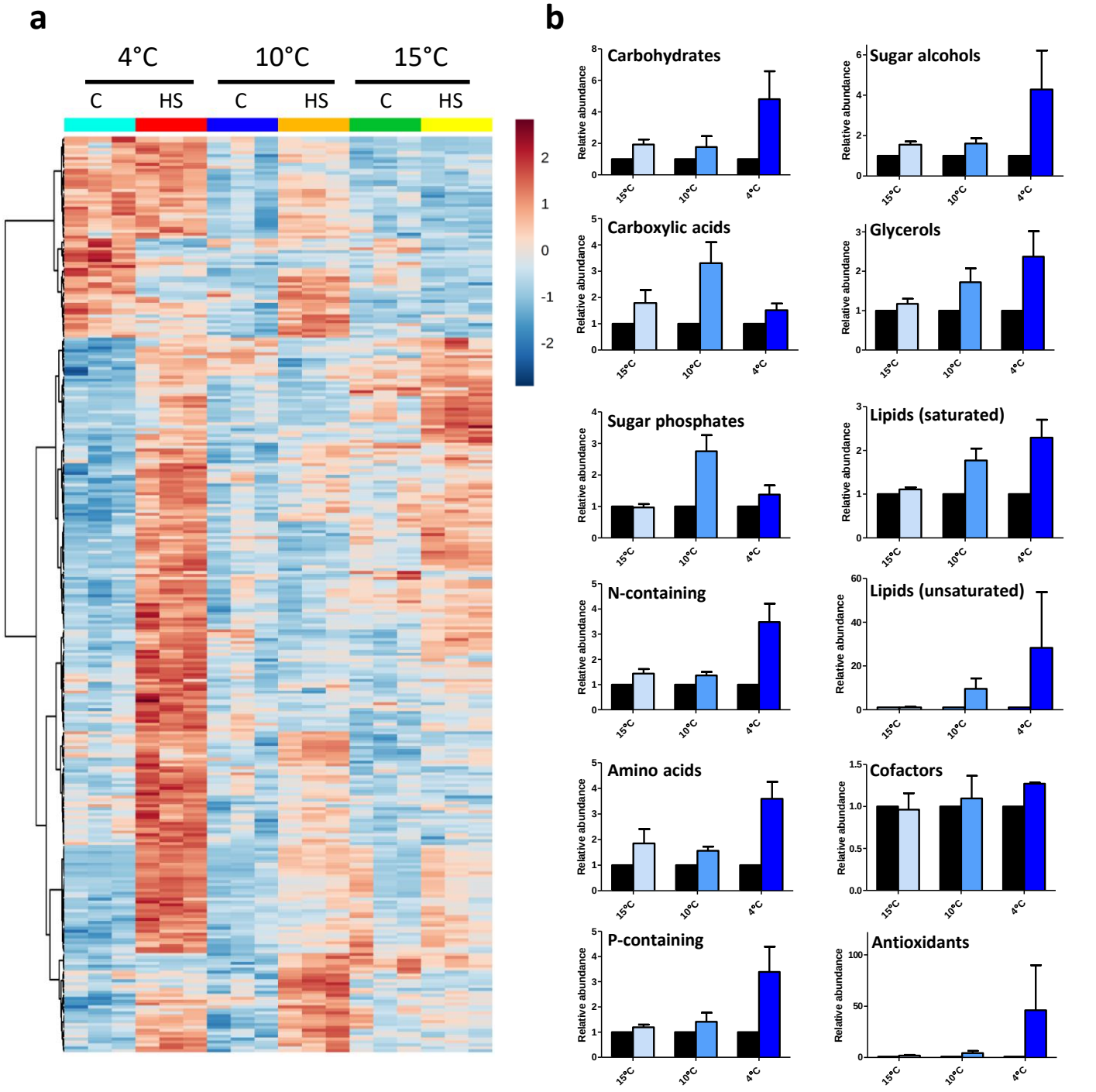


**Figure 6.** Differences in the primary metabolome in UWO241 acclimated at different temperatures (4°C, 10°C, 15°C) and subsequently exposed to heat stress (24°C) for 6 hours. (**a**) Heat map showing the relative changes in metabolite abundances between control samples at each steady-state growth temperature (C) and heat-treated samples (HS). Only metabolites that are significantly different are shown (314 metabolites, ANOVA, $P<0.01$). Three biological replicates are represented using a color-based metabolite profile as indicated (red – high abundance; blue – low abundance). Hierarchical clustering is based on Euclidean distances and Ward's linkage (**b**) Relative abundance of metabolites classified based on their chemical nature. Only metabolites which were positively identified based on their GC-MS spectra and retention times were taken into consideration. In this analysis, the metabolite abundance in algae grown at the three different steady state temperatures were arbitrarily set to 1 (black bars) and all the heat stress treatments were compared to the corresponding control sample (blue bars).

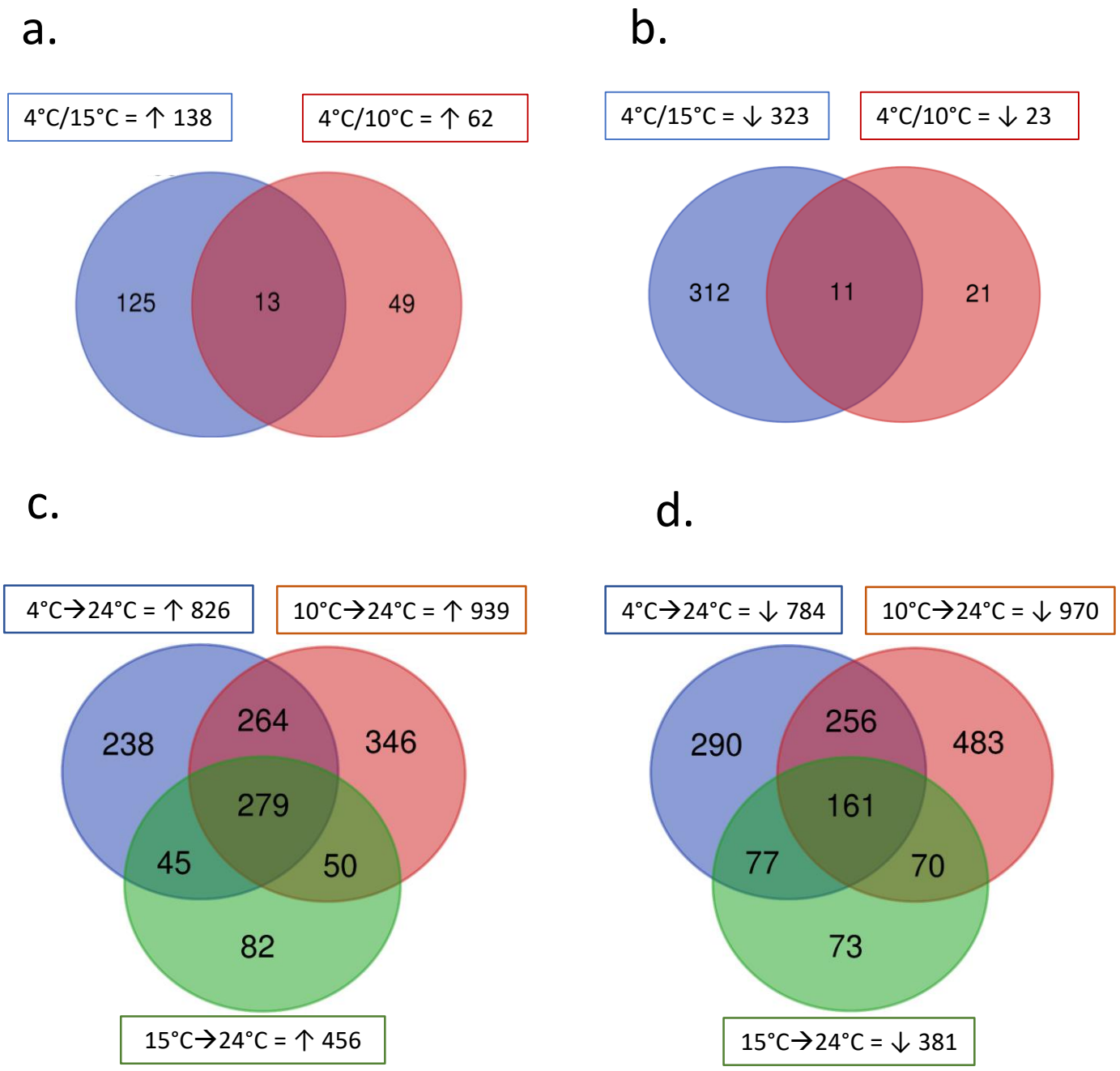


**Figure 7:** Venn diagram indicating intersection of significantly up- **(a)** and down-regulated **(b)** differentially expressed genes (DEGs) in UWO241 grown at 4°C, 10°C and 15°C. In this case, gene expression in the 4°C-grown UWO241 cultures were compared with 15°C (blue, on the left) and 10°C (red, on the right). The number above indicates the total number of up- or down-regulated DEGs in that treatment. Venn diagrams indicating the intersection of significantly **(c)** Up- and **(d)** Down-regulated transcripts in UWO241 grown at 4°C (blue), 10°C (red) and 15°C (green) and exposed to non permissive temperature (24°C) for 6 hours. The number besides the diagram indicates the total number of differentially expressed DEGs in that treatment. In all cases, DEGs have a Fold Change > 4, p-value < 0.05 in three biological replicates.

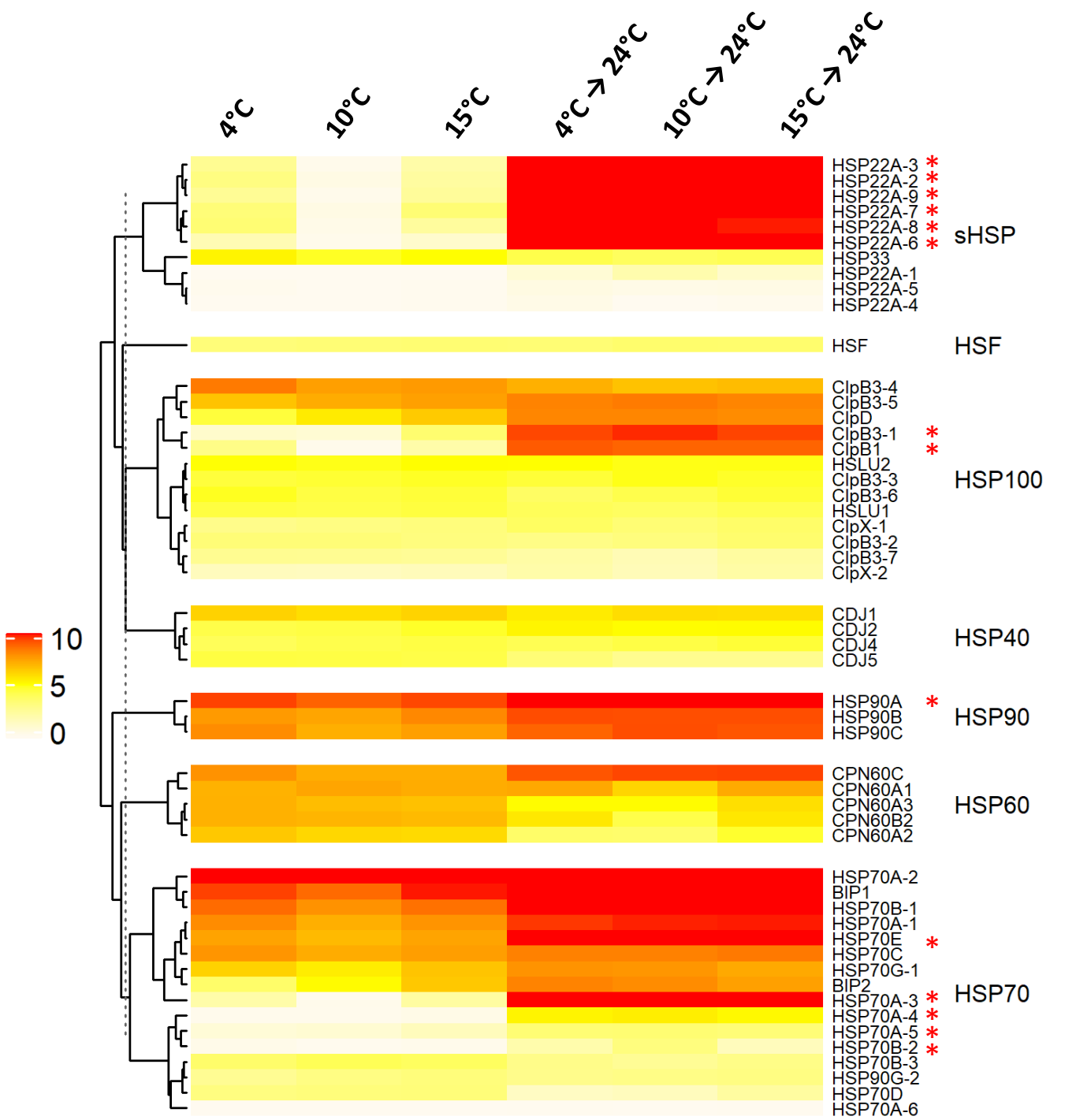


**Figure 8:** Expression of Heat Shock Protein genes in UWO241 grown at three different temperatures (4°C 10°C and 15°C) and exposed heat stress (24°C) for 6 hours. The average FPKM values of gene expression in three biological replicates are represented using a color-based expression profile as indicated (white – low abundance; red – high abundance). All genes encoding putative HSP genes in the UWO241 genome are shown. The genes with a significantly higher expression (FC>4, $p<0.05$) when compared to the corresponding control treatment (e.g., 4°C control compared to 4°C→24°C heat stressed sample) are highlighted with a red asterisk (*). Only genes that are significantly regulated in all three heat shock treatments are highlighted

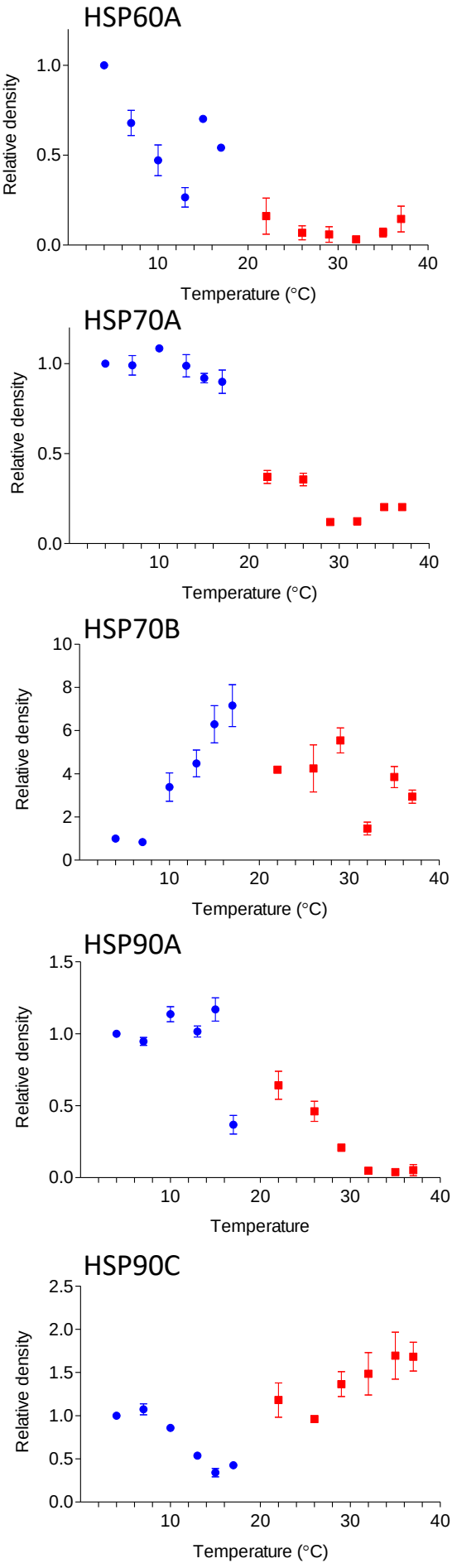


**Figure 9:** Densitometry analysis of the relative HSP abundance determined by Western blotting in cultures of UWO241 (blue) and C. reinhardtii (red) acclimated to different steady-state temperatures. The protein abundance in the 4°C-grown UWO241 was used as the basis of comparison for the relative abundance of HSPs in the other samples. In all cases, the results are the mean of 3 replicates (± SD).

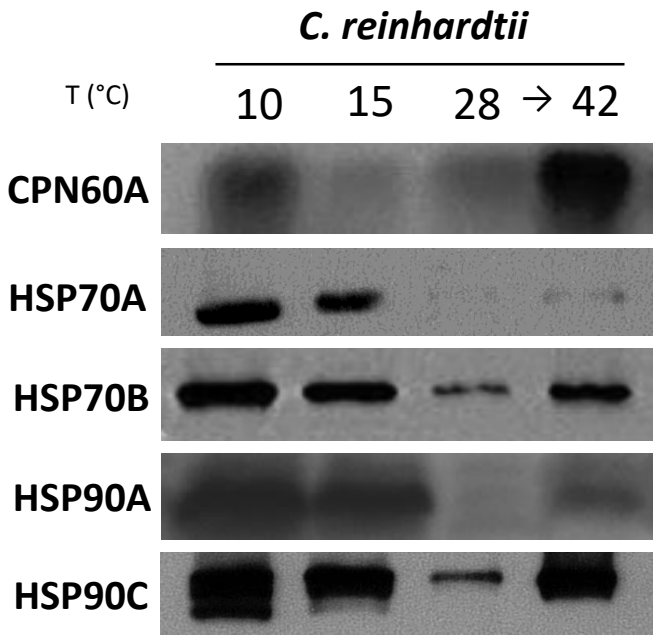


**Figure 10:** HSPs in *C. reinhardtii* acclimated to a steady-state low temperatures (10°C and 15°C) accumulate at comparable levels to those in cultures acclimated to 28°C and exposed to 42°C for 6 hours. The data shown reflect typical results of three biological replicates.

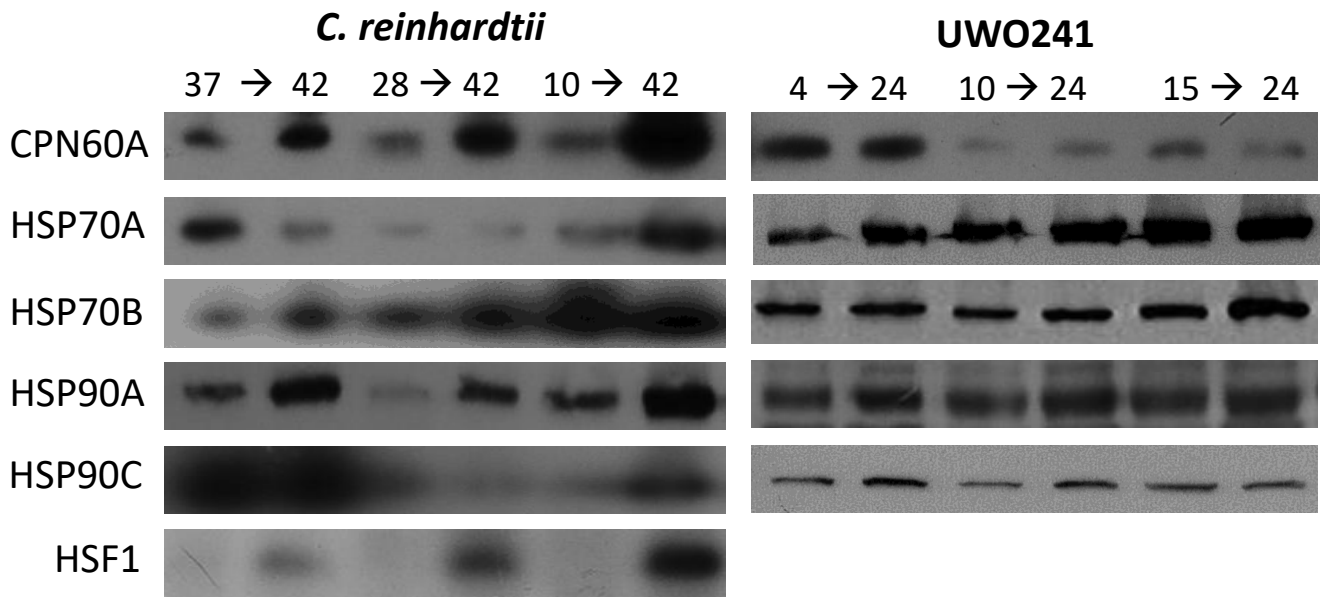


**Figure 11:** Accumulation of Heat Shock proteins in cultures of UWO241 and *C. reinhardtii* cultured under different temperature regimes until mid-log stage (37°C, 28°C and 10°C for *C. reinhardtii*; 15°C, 10°C and 4°C for UWO241) and exposed to 6 hours of heat stress at 42°C for *C. reinhardtii* and 24°C for UWO241. Due to differences in the initial HSP amount between the two species, the immunoblots were exposed and imaged at different intensities in order to capture the change in HSP accumulation between the control and heat stressed samples. The data shown here reflect typical results of three biological replicates. It should be noted that HSF1 could not be detected at the protein level in UWO241

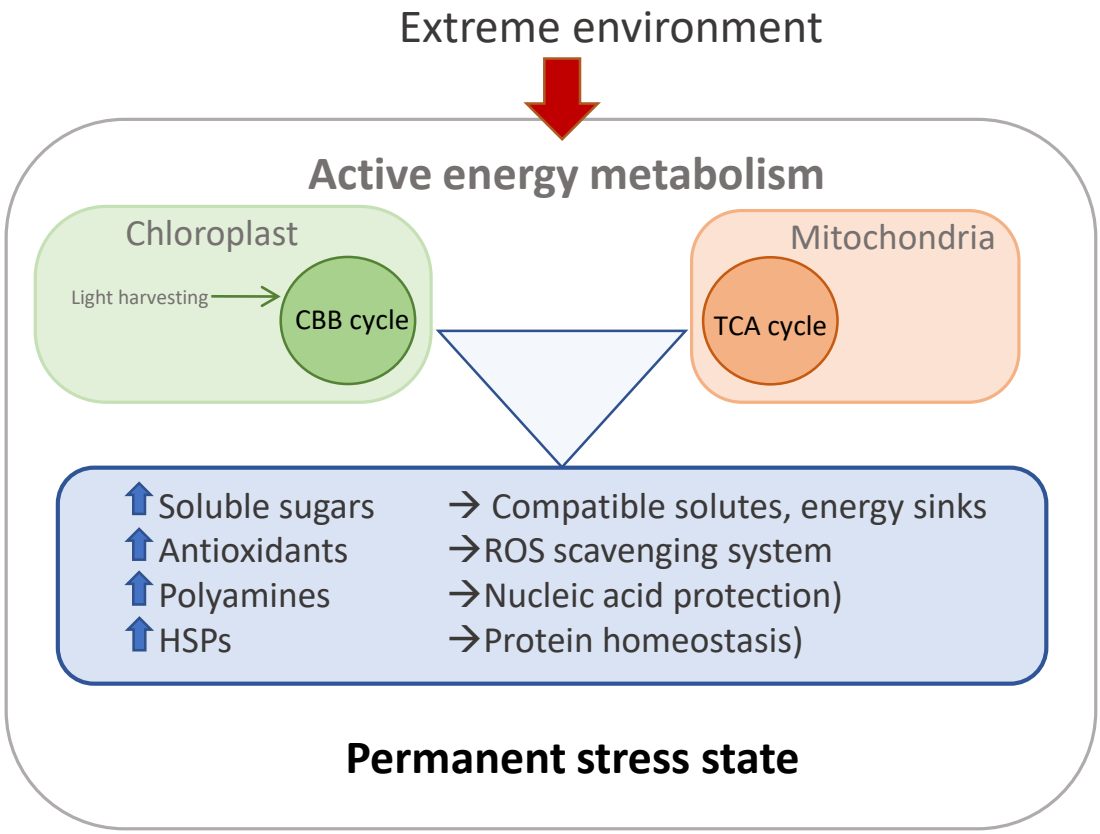


**Figure 12:** The psychrophilic alga UWO241 is adapted to life at low but very stable temperatures of 4-6°C year-round in Lake Bonney, Antarctica. Its physiology at low temperature is characterized by efficient photosynthetic rates comparable to those of *C. reinhardtii* at 25–35°C. (Pocock et al, 2011) and an active energy metabolism characterized by increased accumulation of CBB and TCA cycle intermediates. This active central metabolism fuels a constitutive accumulation of metabolites and proteins important for life at low temperatures, including soluble sugars, antioxidants, polyamines and molecular chaperones that ensure efficient protein folding at low temperatures. We propose that this permanent metabolic stress state provides UWO241 with the ability to cope with its extreme environment, but it also might impede its ability to finely manipulate the metabolic and molecular network in order to cope with additional environmental stressors.